JOURNAL OF COMPUTATIONAL PHYSICS 108, 153–158 (1993)

A Strategy for the Efficient Simulation of Viscous Compressible Flows Using a Multi-domain Pseudospectral Method

PATRICK HANLEY

University of Connecticut, Box U-139ME, Storrs, Connecticut 06269-3139

Received December 5, 1991; revised October 19, 1992

A new multi-domain pseudospectral method is developed to simulate viscous compressible flow in a quasi-one-dimensional nozzle. The flow variables at the interface points are advanced in time using the same second-order time marching scheme as the interior points. The spatial derivatives of the inviscid flux vector are evaluated at the interface points using a spectrally accurate modification of Van Leer's flux vector splitting method. The derivatives of the viscous flux vector are evaluated alternately from neighboring sub-domains. The scheme is found to be spectrally accurate. Shock waves are resolved without oscillations for moderate Reynolds Numbers.

1. INTRODUCTION

Pseudospectral methods are accurate numerical solution techniques for fluid flows which exhibit exponential convergence for smooth flow fields [1, 2]. Advantages such as improved CPU run times, application to complex geometries, and implementation on parallel computers can be realized by dividing the pseudospectral computational domain into smaller regions [3–6]. Pseudospectral methods, however, are currently not widely applied to simulations of compressible fluid flows because of the difficulties encountered in treating shock waves [7]. Shocks can be captured by incorporating an artificial viscosity similar to that of finite difference schemes into the solution [8]. This treatment, however, tends to deteriorate the spectral accuracy of the solution. A 1987 report by Macaraeg, Streett, and Hussaini [9] showed that multi-domain pseudospectral methods can be used to resolve shock waves without adding non-physical artificial viscosity. These shock waves are not discontinuities but rather regions of rapid change whose width depends on the Reynolds number. The shock wave location can be found adaptively using methods similar to that of Ref. [10]. Macaraeg *et al.* further showed that the presence of implicit or explicit artificial viscosity in numerical schemes can adversely affect the physical solution. Simulations free of the inaccuracies caused by artificial viscosity can be used to resolve not only chemically reacting flows but can also be used to accurately study compressible turbulence [11, 12]. A flexible multi-domain pseudospectral methods can be used to extend these compressible viscous flow simulations to practical engineering geometries.

This paper reiterates usefulness of pseudospectral methods for resolving viscous shocks. An efficient multi-domain method for the Navier–Stokes equations is presented which reduces the number of operations needed to treat the inviscid and viscous flux vectors at interface points. The scheme in Ref. [4] imposes continuity of the state variables and flux vector at the interface points. This interface treatment results in a system of equations for the flow variables which can be large if there are a large number of sub-domains. Other multi-domain schemes for compressible flows do not address the viscous flux term in the Navier–Stokes equations. The present multi-domain scheme is used to solve the quasi-one-dimensional Navier–Stokes equations for transonic flows in a nozzle. A second-order time marching method is used to advance the state variables at interior and interface points. The spatial derivatives at the interface points are evaluated using the flux vector splitting technique of Van Leer [13] for the inviscid flux vector and a variation of the alternating domain method of Hanley [6] for the viscous flux vector. The Van Leer split admits a smooth transition of the inviscid flux vector across stagnation and sonic points. Efficiency of the method is enhanced by using the split flux vector to evaluate the derivative only at the interface points. The derivatives at the interior points are evaluated using the original unsplit flux vector. This method is similar to multi-domain techniques found in [5, 14] which are akin to the methods of characteristics. The operational count for evaluating the derivatives of the viscous flux vector at the interface points is negligible. The overall multi-domain scheme for the Navier–Stokes equations is efficient and simple to program and is directly transferable to two- and three-dimensional problems. Results show that the pseudospectral multi-domain scheme can resolve sharp

0021-9991/93 $5.00

shocks using the physical viscosity of the problem. The multi-domain treatment produces exponentially convergent results.

2. GOVERNING EQUATIONS

The governing equation for quasi-one-dimensional compressible viscous flows are given by

$$\frac{\partial U}{\partial t}+\frac{\partial F}{\partial x}+H=\frac{\partial G}{\partial x}, \tag{1a}$$

where

$$U=\begin{bmatrix}\rho A\\ \rho uA\\ \rho EA\end{bmatrix} \tag{1b}$$

$$F=\begin{bmatrix}\rho uA\\ (\rho u^2+p)A\\ \rho uH_h A\end{bmatrix} \tag{1c}$$

$$G=\begin{bmatrix}0\\ \frac{4}{3}A\mu u_x\\ \frac{Ak}{c_v}E_x+\left(\frac{4}{3}A\mu-\frac{Ak}{c_v}\right)uu_x\end{bmatrix} \tag{1d}$$

$$H=\begin{bmatrix}0\\ -p\dfrac{\partial A}{\partial x}\\ 0\end{bmatrix}, \tag{1e}$$

where $E=e+u^2/2$, $H_h=E+p/\rho$, c_v, and c_p is the specific heats at constant volume and pressure, and $A(x)$ is the cross-sectional area of the nozzle. The coefficient of viscosity and thermal conductivity are given according to the power law

$$\mu\approx\left(\frac{T}{T_0}\right)^n, \qquad k\approx\left(\frac{T}{T_0}\right)^n,$$

where for air $n=0.666$. A Prandtl number given by

$$P_r=\mu c_p/k$$

of 0.75 is used for the computations. The internal energy is given by

$$e=\frac{p}{(\gamma-1)\rho}.$$

Equations (1) are subject to characteristic inflow and outflow boundary conditions. In addition to the characteristic boundary conditions, the back pressure is specified at the nozzle exit. At the nozzle inlet, the total pressure and enthalpy are specified.

3. NUMERICAL METHOD

Equations (1) are integrated in time using a second-order accurate two-step time marching scheme. The computational domain is divided into a number of smaller regions. Each region is joined by a common interface point. The flow variables at the domain interface points are advanced in time using the same second-order time marching method as the interior points. However, the derivatives at the interface points are modified to include physically correct information from the sub-domains to the right and left. The following sections give details of the numerical method.

3.1. Time Marching Scheme

The dependent variables are advanced in time using the following two-step time marching method

$$\bar{U}^{n+1}=U^n-\Delta t\left(\frac{\partial F^n}{\partial x}-\frac{\partial G^n}{\partial x}+H^n\right) \tag{2a}$$

$$U^{n+1}=\frac{1}{2}\left(\bar{U}^{n+1}+U^n-\Delta t\left(\frac{\partial \bar{F}^{n+1}}{\partial x}-\frac{\partial \bar{G}^{n+1}}{\partial x}+\bar{H}^{n+1}\right)\right). \tag{2b}$$

The following section describes the scheme for evaluating the spatial derivatives.

3.2. Spatial Derivatives

The computational domain can be divided into a number of smaller regions or zones. Neighboring sub-domains share a common interface point. Each of these regions can be mapped to the interval $-1\leqslant\xi\leqslant 1$ which can be discretized by a Chebyshev polynomial on Gauss–Labatto points given by

$$\xi_j=\cos\left(\frac{\pi j}{N}\right). \tag{3}$$

The Chebyshev pseudospectral derivative operator D for each of the sub-domains is a full matrix. The elements of the matrix are given in Ref. [1] as

$$d_{jk}=\begin{cases}\dfrac{c_k}{c_j}\dfrac{(-1)^{j+k}x}{x_k-x_j} & \text{if } j\neq k\\ \dfrac{x_j}{2(1-x_j^2)} & \text{if } j=k \quad \text{but} \quad 0\leqslant j\leqslant N\\ \dfrac{2N^2+1}{6} & \text{if } j=k=0\\ -\dfrac{2N^2+1}{6} & \text{if } j=k=N,\end{cases} \tag{4}$$

where x_j is given by Eq. (3) and $c_j=2$ if $j=0$ or $j=N$, otherwise $c_j=1$. For the computations, D is further modified so that x_0 refers to the leftmost point while x_N refers to the rightmost point of the sub-domain. The modification also takes into account the linear transformation. Both D and N can vary for one domain to the next.

Approximating first derivatives at all points in a sub-domain with N elements will require N^2 operations. A fast Fourier transform can be used to reduce the operational count to $N\log N$; however, the technique is complex to program and no significant advantage is realized until N approaches a large number [15]. The matrix multiplication is used in this paper because the number of modes in the pseudospectral sum will be relatively small. Evaluating the spatial derivatives at the interior and interface points requires different treatments which are covered in the next sections.

3.2.1. *Interior Points*

The spatial derivatives in Eq. (2) can be evaluated at all time levels in each sub-domain using

$$\frac{\partial F_j}{\partial x}=\sum_{n=0}^{N} d_{jn}F(x_n) \tag{5}$$

and

$$\frac{\partial G_j}{\partial x}=\sum_{n=0}^{N} d_{jn}G(x_n), \tag{6}$$

where E_x and u_x are given by

$$\frac{\partial E_j}{\partial x}=\sum_{n=0}^{n=N} d_{jn}E(x_n) \tag{7}$$

$$\frac{\partial u_j}{\partial x}=\sum_{n=0}^{N} d_{jn}u(x_n). \tag{8}$$

3.2.2. *Interface Points*

The derivatives of the inviscid and viscous flux vectors are treated separately at the interface points. Figure 1 shows two neighboring sub-domains with a common interface point. The subscripts left, right, interface refer to quantities in the left, right sub-domains and the interface point, respectively.

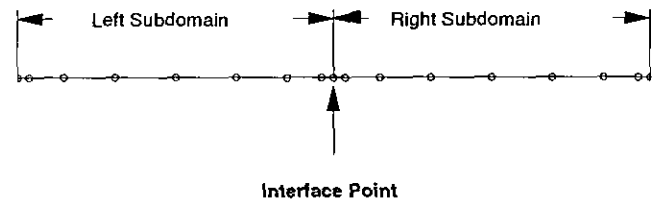

FIG. 1. Two neighboring pseudospectral domains.

Inviscid Fluxes. First derivatives can be computed at interface points using the technique of flux-vector splitting described in [13] for the inviscid flux at all time levels. The flux vector at the interface points can be split into two parts, F^+ and F^-, which represent right and left running waves. The derivative $\partial F/\partial x$ (for a flow from left to right) can be represented at the interface point of two neighboring domains as

$$\left(\frac{\partial F}{\partial x}\right)_{\text{interface}}=\left(\frac{\partial F^+}{\partial x}\right)_{\text{left}}+\left(\frac{\partial F^-}{\partial x}\right)_{\text{right}}, \tag{9}$$

where $F^\pm$ is given in [13] as

$$F^\pm=\begin{bmatrix}\pm\rho a\{\frac{1}{2}(M\pm 1)\}^2 A\\ f_1^\pm\dfrac{(\gamma-1)u\pm 2a}{\gamma}A\\ f_1^\pm\dfrac{\{(\gamma-1)u\pm 2a\}^2}{2(\gamma^2-1)}A\end{bmatrix} \quad \text{for} \quad M<1 \tag{10}$$

and

$$f_1^\pm=\pm\rho a\{\tfrac{1}{2}(M\pm 1)\}^2 \tag{11}$$

If $M>1$ then $F^+=F$ and $F^-=0$.

The flux vector splitting is used to compute the first derivative of F only at the interface points. It is still necessary to compute the split fluxes at all interior points to evaluate the pseudospectral derivative. The operational count for computing $\partial F/\partial x$ at the interface point is about the same as an interior point, i.e., $O(N)$.

Viscous Fluxes. Reference [6] was successful in using an alternating domain technique for computing second derivatives at the domain interface. It was shown in [16] by numerical experiments that eigenvalues of this second derivative operator for two domains (with equal and unequal numbers of points) were negative. Negative eigenvalues of the derivative operator are necessary for the temporal stability of a numerical scheme. The scheme was also

found to be exponentially convergent for the one-dimensional heat equation. A variation of this technique is used below to compute the derivative of the viscous flux at the interface points.

For the predictor step, first compute u_x and E_x in all of the sub-domains from Eqs. (8) and (7). Assign the value of $(u_x(x_N))_{\text{left}}$ and $(E_x(x_N))_{\text{left}}$ of each sub-domain to the interface point so that

$$(u_x)_{\text{interface}} = (u_x(x_0))_{\text{right}} = \left(\sum_{j=0}^{N} d_{Nj} u(x_j)\right)_{\text{left}} \quad (12)$$

$$(E_x)_{\text{interface}} = (E_x(x_0))_{\text{right}} = \left(\sum_{j=0}^{N} d_{Nj} E(x_j)\right)_{\text{left}}. \quad (13)$$

The derivative of the viscous flux can then be computed using

$$(G_x)_{\text{interface}} = (G_x(x_N))_{\text{left}} = \left(\sum_{j=0}^{N} d_{0j} G(x_j)\right)_{\text{right}}. \quad (14)$$

For the corrector step of Eq. (2) first evaluate u_x and E_x in all domains while at the interface points let

$$(u_x)_{\text{interface}} = (u_x(x_N))_{\text{left}} = \left(\sum_{j=0}^{N} d_{0j} u(x_j)\right)_{\text{right}} \quad (15)$$

$$(E_x)_{\text{interface}} = (E_x(x_N))_{\text{left}} = \left(\sum_{j=0}^{N} d_{0j} E(x_j)\right)_{\text{right}}. \quad (16)$$

The derivative of the viscous flux can then be computed using

$$(G_x)_{\text{interface}} = (G_x(x_0))_{\text{right}} = \left(\sum_{j=0}^{N} d_{Nj} G(x_j)\right)_{\text{left}}. \quad (17)$$

The operational count for computing $\partial G/\partial x$ at the interface is the same as an interior point.

4. RESULTS

Results are obtained for a converging diverging nozzle with the cross-sectional area given by

$$A(x) = 1 - 0.8x(1-x), \qquad 0 \leqslant x \leqslant 1.$$

The equations are integrated in time from stagnation conditions to the final steady state. The back pressure to stagnation pressure ratio is set to 0.78. This produces subsonic flow in the converging section of the nozzle with supersonic flow past the throat in the diverging section terminating with a shock at about $x = 0.77$ and subsonic flow at the exit. A total of 12 sub-domains is used to resolve the flow. The

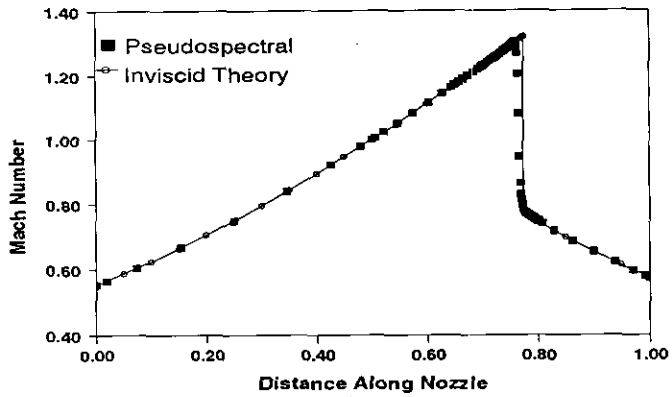

FIG. 2. Mach number in nozzle.

sub-domain interface points are located at $x = 0.5$, 0.65, 0.70, 0.72, 0.74, 0.75, 0.76, 0.77, 0.78, 0.79, 0.80. Numerical experiments are performed for 5, 7, 9, and 11 points per sub-domain. A fine grid is used for a relatively large area around the final position of the shock to capture the evolving shock wave. An adaptive scheme similar to that of Ref. [10 or 17] can be used to improve the efficiency of the computations by automatically locating the shock position. In addition, a standard MacCormack scheme is used to solve Eq. (1) in order to compare the pseudospectral results. Solutions are obtained for 801, 1601, and 3201 evenly spaced points. All the computations are performed for a Reynolds number of 2000 (based on stagnation sound speed and channel length). Figure 2 shows a comparison of the computed solution with the solution obtained by using exact inviscid theory [18]. The computed solution is in good agreement with the inviscid calculations even for this relatively low Reynolds number example. Figure 3 is a plot of the nine points/domain solution compared with the 1601 equally spaced points MacCormack's solution in the shock layer region. The figure shows that the multi-domain technique is in excellent agreement with the finite difference method and is proof that the multi-domain scheme works in this viscous dominated region of the flow.

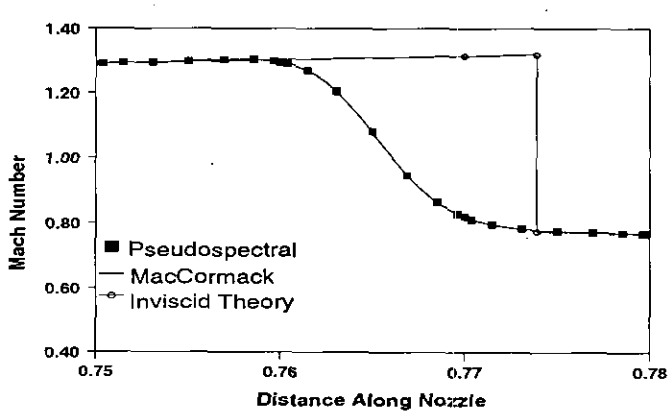

FIG. 3. Mach number in thin viscous layer.

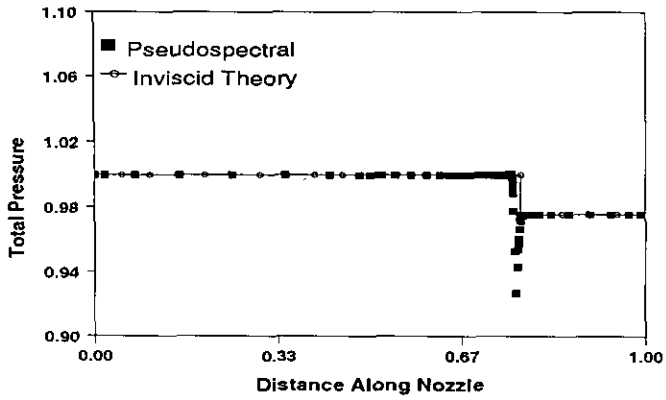

FIG. 4. Total pressure in nozzle normalized with respect to the ambient total pressure.

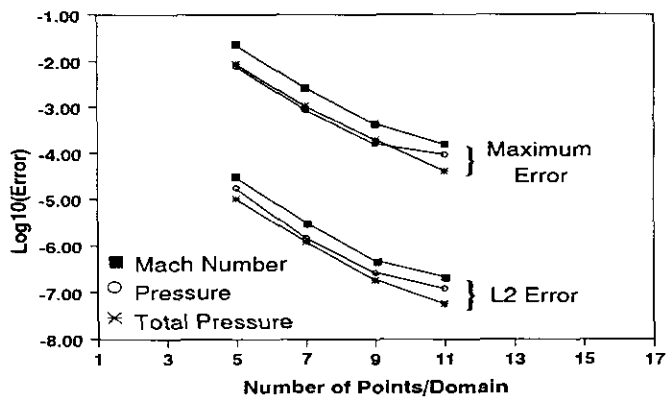

FIG. 6. Convergence of the multi-domain method for Mach number and pressure and total pressure.

Figure 4 shows the total pressure using the pseudospectral scheme (nine points/domain) compared to the exact inviscid theory. Again, there is good agreement between the inviscid and viscous theory for a Reynolds Number of 2000. Figure 5 shows an enlargement of the viscous region showing the results of the pseudospectral scheme and the MacCormack's method. Both solutions exhibit excellent agreement and show an undershoot in the total pressure. This non-physical behavior was also observed by Morduchow *et al.* [19] in an analytical study of one-dimensional viscous compressible flows.

A spatial convergence study is performed for the pseudospectral multi-domain method for the transonic nozzle. The 3201 points MacCormack's method is used as the "exact" solution. This results in 96 points in the viscous dominated region between $x = 0.75$ and $x = 0.78$. Figure 6 is a plot of the convergence of the maximum and L_2 errors with 5, 7, 9, and 11 points in each sub-domain. The straight lines in the graph imply exponential convergence and is evidence of the integrity of the sub-domain technique in both the inviscid and viscous dominated regions of the flow. Figure 6 also shows that the magnitude of the convergence slope for the pseudospectral method begins to decrease between the nine points/sub-domain and 11 points/sub-domain points. This is because the 11 point/sub-domain pseudospectral solution is about the same order of accuracy as the 3201 point MacCormack's solution. Figure 7 is a plot of the convergence of MacCormack method for 801 and 1601 points. The plot shows that the error decreases less than an order of magnitude as the total number of points is doubled. However, the error associated with the pseudospectral method decreases by about an order of magnitude when the number of points in each sub-domain is increased by two. Figures 6 and 7 show that the nine points/sub-domain pseudospectral method provides about the same order of accuracy as the 1601 points MacCormack's method. The maximum error for both methods occurs in the viscous dominated region located at $0.76 \leqslant x \leqslant 0.78$.

Since the integration schemes (for the MacCormack and pseudospectral methods) are time accurate, all solutions converge at about the same physical times (about 0.5 s). However, the number of iterations required for convergence can vary for each computation. This is because the maxi-

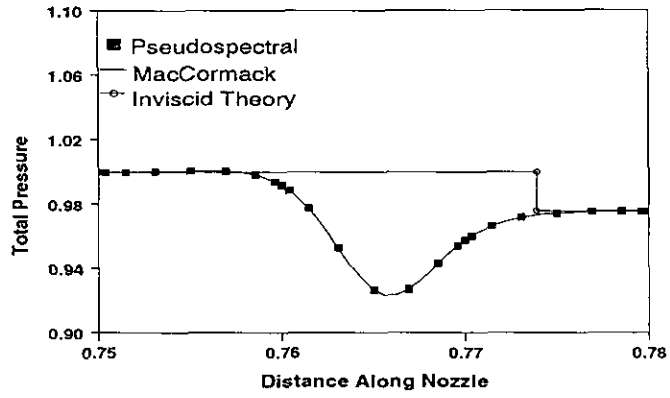

FIG. 5. Total pressure in viscous layer normalized with respect to the ambient total pressure.

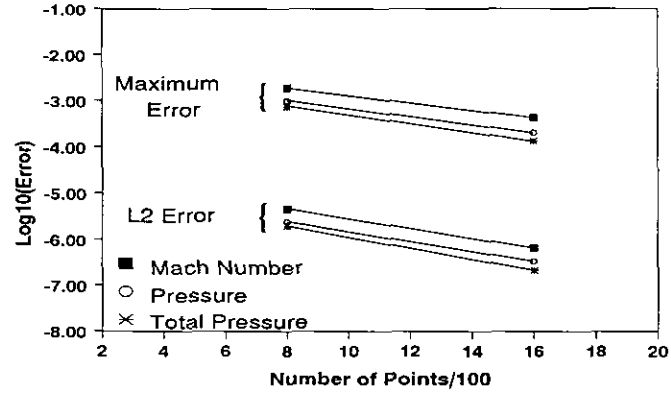

FIG. 7. Convergence of the MacCormack's method for Mach number and pressure and total pressure.

TABLE I

Multi-domain Pseudospectral Method (12 Sub-domains)

# Points/domain	Time step	CPU time/iteration	CPU for convergence
7	2×10^{-7} s	6.798×10^{-3} s	283.25 min
9	1×10^{-7} s	9.076×10^{-3} s	756.33 min
11	5×10^{-8} s	1.15×10^{-2} s	1,916.67 min

mum global allowable time step for stability was used to advance the computations. This time was determined by manually dividing the time step by two until a stable solution was reached. Tables I and II show the statistics for the computations for both the pseudospectral and MacCormack's methods on a RISC 6000/320H computer.

Since the accuracy of the nine points/domain and the 1601 points MacCormack solutions are comparable, the results in Tables I and II suggest that the pseudospectral scheme decreases the computation time by a factor of seven. As more resolution is required in the viscous shock layer, the pseudospectral method will be more efficient compared to MacCormack's method. The 3201 point MacCormack solution would require about 32 days of computation if ambient initial conditions were used. To speed up the computations, the converged nine points/domain pseudospectral solution was projected to the 3201 points using spectral interpolation. An additional 10^6 iterations was performed to obtain the steady solution.

The CPU usage is extensive for the transonic nozzle computation. This is because the shock was resolved using a fine grid and a small time step was required for stability. The extensive CPU usage is expected in direct turbulent simulations, where the fine turbulent scales are about the same order of magnitude as the shock thickness. In practical engineering applications, it is advisable to use shock capturing or shock fitting [20] in conjunction with the domain decomposition scheme for flows with shock waves.

5. CONCLUSIONS

An efficient multi-domain scheme is devised for viscous compressible flows. The scheme avoids extra equations and conditions to solve for the unknowns at the interface points. The method is directly applicable to two- and three-dimensional problems if aligning sub-domains are used. For general complex bodies nonaligned domains can be useful. Spectral interpolants can be used for nonaligned domains.

TABLE II

MacCormack's Method

Number of points	Time step	CPU time/iteration	CPU for convergence
801	1×10^{-6} s	6.735×10^{-2} s	561.25 min
1601	2×10^{-7} s	1.387×10^{-1} s	5,780.17 min
3201	5×10^{-8} s	2.817×10^{-1} s	46,950.00 min (projected)

ACKNOWLEDGMENTS

This work was performed under Grant CTS-9010669 from the National Science Foundation monitored by Dr. S. Traugott and Grant NAG3-1280 from NASA Lewis Research Center monitored by Dr. L. Reid. The author thanks Dr. W. L. Harris at the University of Tennessee Space Institute and Professor D. A. Koprova at Florida State University for their contributions.

REFERENCES

1. C. Canuto, M. Y. Hussaini, A. Quarteroni, and T. A. Zang, *Spectral Methods in Fluid Dynamics*, Springer-Verlag, New York, 1987.
2. D. Gottlieb and S. A. Orszag, *Numerical Analysis of Spectral Methods: Theory and Applications*, SIAM-CBMS, Philadelphia, 1977.
3. S. A. Orszag, *J. Comput. Phys.* **37**, No. 70 (1980).
4. M. G. Macaraeg and C. L. Streett, *Appl. Numer. Math.* **2**, 95 (1986).
5. D. A. Kopriva, ICASE Report 86–28, 1986.
6. P. E. Hanley, Ph.D. dissertation, Massachusetts Institute of Technology, Cambridge, MA, 1988 (unpublished).
7. M. Y. Hussaini, D. A. Kopriva, M. D. Salas, and T. A. Zang, *AIAA J.* **23**, 64 (1985).
8. L. Sakell, *AIAA J.* **22**. No. 7 (1984).
9. M. G. Macaraeg, C. L. Street, and M. Y. Hussaini, ICASE Report No. 87–35, 1987.
10. P. E. Hanley, "Adaptive Pseudospectral Solutions of Viscous Flows," in *Proceedings Seventh International Conference on Numerical Methods in Thermal Problems, Stanford, CA, July 8–12th 1991.*
11. T. Passot and A. Pouquet, *J. Fluid Mech.* **181**, 441 (1987).
12. K. Dang and P. Loisel, "Direct Simulation of Viscous Compressible Transitional Flows," in *Current Trends in Turbulence Research*, edited by H. Barnover, M. Mond, and Y. Unger. Progress in Aeronautics and Aeronautics (AIAA, Washington, DC), Vol. 112.
13. B. Van Leer, ICASE Report No. 82–30, September 28, 1982 (unpublished).
14. A. Quarteroni, ICASE Report No. 89–5, 1989 (unpublished).
15. T. D. Taylor, R. S. Hirsh, and M. M. Nodworny, *Comput. Fluids* **12**, No. 1 (1984).
16. P. Hanley, Spectral-differencing for compressible fluid flows (unpublished).
17. C. Mavriplis, ICASE Report No. 92–36, 1992 (unpublished).
18. J. D. Anderson, *Modern Compressible Flow: With Historical Perspectives*, McGraw–Hill, New York, 1982.
19. M. Morduchow and P. A. Libby, *J. Aeronaut. Sci.* **16**, 674 (1949).
20. D. A. Kopriva, T. A. Zang, and M. Y. Hussaini, *AIAA J.* **29**, No. 9, 1458 (1991).